THE PUBLISHING HOUSE
OF THE ROMANIAN ACADEMY

PROCEEDINGS OF THE ROMANIAN ACADEMY, Series A,
Volume 18, Number 4/2017, pp. 378–385

ON THE SONIC FILMS WITH DEFECTS

Veturia CHIROIU [1], Ligia MUNTEANU [1], Dan DUMITRIU [1], Cristian RUGINA[1], Cornel BRISAN [2]

[1] Institute of Solid Mechanics, Romanian Academy, Dept of Deformable Media and Ultrasonics, Bucharest, Romania
[2] Technical University of Cluj-Napoca, Dept. of Mechatronics and System Dynamics, Cluj-Napoca, Romania
Corresponding author: Veturia CHIROIU, E-mail: veturiachiroiuilie@gmail.com

Abstract. The cnoidal method is used to analyse the behaviour of multilayer films with randomly inserted defects. These structures have a significant potential to architectural acoustics. The film is consisted of alternating layers of material with different mechanical properties, following a triadic Cantor sequence, and despite of its non-periodicity, it behaves like periodic sonic composites with full band-gaps and localised modes around defects. The cnoidal method is furnishing the solutions expressed as a sum of linear and nonlinear superposition of cnoidal waves. The significant evanescent behavior of the film results from more favourable frequencies and spatial matching of coupled modes in the film, leading to widening of the full band gaps.

Key words: multilayer film; cantor sequence; full band-gap; defects; noise control.

1. INTRODUCTION

The inverse scattering transform is extensively used to solve the wave propagation problems [1–4]. The theta-function representation of solutions or cnoidal method is describable as a linear superposition of Jacobi elliptic functions (cnoidal functions) and additional terms, which include nonlinear interactions among them [5].

The cnoidal functions are much richer than the trigonometric or hyperbolic functions, that is, the modulus $0 \le m \le 1$ of the cnoidal function, can be varied to obtain a sine or cosine function, a Stokes function or a solitonic function, sech or tanh [6]. A great deal of work has been done to study the periodic sonic composites which exhibit important features of sonicity such as full band-gaps and localized modes around interfaces. A review of the physical aspects of sonic materials is reported by Miyashita [7]. The full band-gaps in periodic sonic composites are analysed not only in experimental works [8–10], but also in theoretical ones [11–17].

In the presence of defects, sonic structures exhibit significant localized modes and a great evanescent behavior [18–30]. We note that the non-periodicity can also lead to full band-gaps generation [31]. In the multilayer film consisting of alternating layers of different materials following a triadic Cantor sequence, the subharmonic waves are the key for sonicity. An anharmonic coupling between the extended-mode (phonon) and the localized-mode (fracton) vibration regimes explained this phenomenon.

Allipi [32], Alippi *et al*. [33, 34] and Craciun *et al*. [35] put into evidence the extremely low thresholds for subharmonic waves in artificial piezoelectric plates with Cantor-like structure, as compared to the corresponding homogeneous and periodical plates. They demonstrate that the large enhancement of non-linear interaction results from the spatial matching of coupled fractons and phonons modes. The existence of multiple fracton and phonon modes in the displacement field was analyzed by Scalerandi *et al.* [36] and Chiroiu *et al.* [37].

This paper is organized as follows: In section 2 the cnoidal method is shortly presented. In the section 3, the model of the film with defects is described. The analytical solutions of the equations are derived by using the cnoidal method. The numerical results and discussion are also presented. We show that the presence of defects breaks the symmetry of the waves and widens the size of band-gaps. The role of the rotational angle of the square defects on the distribution of localized modes is investigated. Finally, the Section 4 contains the conclusions.

2. THE CNOIDAL METHOD

This method requires brief information necessary to describe the cnoidal waves [5]. The arc length of the ellipse is related to the integral $E(z)=\int_0^z \frac{\sqrt{(1-k^2x^2)}\mathrm{d}x}{\sqrt{(1-x^2)}}$, with $0<k<1$. Another elliptical integral is given by $F(z)=\int_0^z \frac{\mathrm{d}x}{\sqrt{(1-x^2)(1-k^2x^2)}}$. The integrals $E(z)$ and $F(z)$ are Jacobi elliptic integrals of the first and the second kinds. Jacobi inspired by Gauss, discovered in 1820 that the inverse of $F(z)$ is an elliptical double-periodic integral $F^{-1}(\omega)=\mathrm{sn}(\omega)$. Jacobi compares the integral

$$v=\int_0^{\varphi}\frac{\mathrm{d}\theta}{(1-m\sin^2\theta)^{1/2}}, \tag{1}$$

where $0\le m\le 1$, to the elementary integral

$$w=\int_0^{\varphi}\frac{\mathrm{d}t}{(1-t^2)^{1/2}}, \tag{2}$$

and observed that (2) defines the inverse of the trigonometric function sin if we use the notations $t=\sin\theta$ and $\psi=\sin w$. He defines a new pair of inverse functions from (1)

$$\mathrm{sn}\,v=\sin\varphi,\ \mathrm{cn}\,v=\cos\varphi. \tag{3}$$

These are two of the Jacobi elliptic functions, usually written $\theta_{lin}(\eta)=\frac{2}{\lambda}\frac{\partial^2}{\partial x^2}\log G(\eta)$ and $\mathrm{cn}(v,m)$ to denote the dependence on the parameter m. The angle φ is called the amplitude $\varphi=\mathrm{am}\,u$. We also define the Jacobi elliptic function $\mathrm{dn}v=(1-m\sin^2\varphi)^{1/2}$. For $m=0$, we have
$v=\varphi$, $\mathrm{cn}(v,0)=\cos\varphi=\cos v$,

$$v=\varphi\ \ \mathrm{sn}(v,0)=\sin\varphi=\sin v,\ \mathrm{dn}(v,0)=1, \tag{4}$$

and for $m=1$

$$v=\mathrm{arcsech}(\cos\varphi),\ \mathrm{cn}(v,1)=\mathrm{sech}v,$$

$$\mathrm{sn}(v,1)=\tanh v,\ \mathrm{dn}(v,1)=\mathrm{sech}v. \tag{5}$$

The functions $\mathrm{sn}\,v$ and $\mathrm{cn}\,v$ are periodic functions with the period $\int_0^{2\pi}\frac{\mathrm{d}\theta}{(1-m\sin^2\theta)^{1/2}}=4\int_0^{\pi/2}\frac{\mathrm{d}\theta}{(1-m\sin^2\theta)^{1/2}}$. The later integral is the complete elliptic integral of the first kind $K(m)=\int_0^{\pi/2}\frac{\mathrm{d}\theta}{(1-m\sin^2\theta)^{1/2}}$. The period of the function $\mathrm{dn}\,v$ is $2K$. For $m=0$ we have $K(0)=\pi/2$. For increasing of m, $K(m)$ increases monotonically $K(m)\approx\frac{1}{2}\log\frac{16}{1-m}$. Thus, this periodicity of $\mathrm{sn}(v,1)$ and $\mathrm{cn}(v,1)=\mathrm{sech}v$ is lost for $m=1$, so $K(m)\to\infty$. Some relations between the cnoidal functions are given below

$$\mathrm{cn}^2+\mathrm{sn}^2=1,\ \mathrm{dn}^2+m\,\mathrm{sn}^2=1,\ \frac{\mathrm{d}}{\mathrm{d}v}\mathrm{cn}=-\mathrm{sn}\,\mathrm{dn},$$

$$\frac{\mathrm{d}}{\mathrm{d}v}\mathrm{sn}=\mathrm{cn}\,\mathrm{dn},\ \frac{\mathrm{d}}{\mathrm{d}v}\mathrm{dn}=-m\,\mathrm{sn}\,\mathrm{cn},$$

where the argument v and parameter m are the same throughout relations.

Consider now the nonlinear system of equations that govern the motion of a sonic structure

$$\frac{\mathrm{d}\theta_i}{\mathrm{d}t} = F_i(\theta_1, \theta_2, ..., \theta_n), \quad i = 1, ..., n, \quad n \geq 3, \tag{6}$$

with $x \in \mathrm{R}^n$, $t \in [0, T]$, $T \in \mathrm{R}$, where F may be of the form

$$\begin{aligned} F_i = &\sum_{p=1}^{n} a_{ip}\theta_p + \sum_{p,q=1}^{n} b_{ipq}\theta_p\theta_q + \sum_{p,q,r=1}^{n} c_{ipqr}\theta_p\theta_q\theta_r + \\ &+ \sum_{p,q,r,l=1}^{n} d_{ipqrl}\theta_p\theta_q\theta_r\theta_l + \sum_{p,q,r,l,m=1}^{n} e_{ipqrlm}\theta_p\theta_q\theta_r\theta_l\theta_m + \ldots, \end{aligned} \tag{7}$$

with $i = 1, 2, ..., n$, and $a, b, c...$ constants.

The system of equations (6) has the remarkable property that it can be reduced to Weierstrass equations. The cnoidal method is suitable to solve the equations (6). To simplify the presentation, let us omit the index i and note the solution by $\theta(t)$.

We introduce the function transformation

$$\theta = 2\frac{\mathrm{d}^2}{\mathrm{d}t^2}\log\Theta_n(t), \tag{8}$$

where the theta function $\Theta_n(t)$ are defined as

$$\Theta_1 = 1 + \exp(\mathrm{i}\omega_1 t + B_{11}),$$

$$\Theta_2 = 1 + \exp(\mathrm{i}\omega_1 t + B_{11}) + \exp(\mathrm{i}\omega_2 t + B_{22}) + \exp(\omega_1 + \omega_2 + B_{12}),$$

$$\begin{aligned} \Theta_3 = &1 + \exp(\mathrm{i}\omega_1 t + B_{11}) + \exp(\mathrm{i}\omega_2 t + B_{22}) + \\ &+ \exp(\mathrm{i}\omega_3 t + B_{33}) + \exp(\omega_1 + \omega_2 + B_{12}) + \\ &+ \exp(\omega_1 + \omega_3 + B_{13}) + \exp(\omega_2 + \omega_3 + B_{23}) + \\ &+ \exp(\omega_1 + \omega_2 + \omega_3 + B_{12} + B_{13} + B_{23}), \end{aligned} \tag{9}$$

and

$$\Theta_n = \sum_{M \in (-\infty, \infty)} \exp(\mathrm{i}\sum_{i=1}^{n} M_i\omega_i t + \frac{1}{2}\sum_{i<j}^{n} B_{ij}M_iM_j), \tag{10}$$

$$\exp B_{ij} = \left(\frac{\omega_i - \omega_j}{\omega_i + \omega_j}\right)^2, \quad \exp B_{ii} = \omega_i^2. \tag{11}$$

Further, we write the solution (8) under the form

$$\theta(t) = 2\frac{\partial^2}{\partial t^2}\log\Theta_n(\eta) = \theta_{lin}(\eta) + \theta_{int}(\eta), \tag{12}$$

for $\eta = -\omega t + \phi$. The first term θ_{lin} represents, as above, a linear superposition of cnoidal waves. Indeed, after a little manipulation and algebraic calculus, (12) gives

$$\theta_{lin} = \sum_{l=1}^{n} \alpha_l \left[\frac{2\pi}{K_l\sqrt{m_l}} \sum_{k=0}^{\infty} \left(\frac{q_l^{k+1/2}}{1 + q_l^{2k+1}} \cos(2k+1)\frac{\pi\omega_l t}{2K_l}\right)^2\right]. \tag{13}$$

In (13) we recognize the expression [6]

$$\theta_{lin} = \sum_{l=1}^{n} \alpha_l \mathrm{cn}^2[\omega_l t; m_l], \tag{14}$$

with

$$q = \exp(-\pi \frac{K'}{K}), \; K = K(m) + \int_0^{\pi/2} \frac{\mathrm{d}u}{\sqrt{1 - m\sin^2 u}},$$

$$K'(m_1) = K(m), \;\; m + m_1 = 1.$$

The second term θ_{int} represents a nonlinear superposition or interaction among cnoidal waves. We write this term as

$$2\frac{\mathrm{d}^2}{\mathrm{d}t^2}\log[1 + \frac{F(t)}{G(t)}] \approx \frac{\beta_k \mathrm{cn}^2(\omega t, m_k)}{1 + \gamma_k \mathrm{cn}^2(\omega t, m_k)}. \tag{15}$$

If m_k take the values 0 or 1, the relation (15) is directly verified. For $0 \le m_k \le 1$, the relation is numerically verified with an error of $|e| \lesssim 5 \times 10^{-7}$. Consequently, we have

$$\theta_{int}(x,t) = \frac{\sum_{k=0}^{n} \beta_k \mathrm{cn}^2[\omega_k t; m_k]}{1 + \sum_{k=0}^{n} \lambda_k \mathrm{cn}^2[\omega_k t; m_k]}. \tag{16}$$

As a result, the cnoidal method yields to solutions consisting of a linear superposition and a nonlinear superposition of cnoidal waves.

3. THE SONIC STRUCTURE WITH DEFECTS

The film consists of alternating layers of piezoelectric ceramics (PZ) and the epoxy resin (ER), following a triadic Cantor sequence with 31 elements as the host [31]. The length of the plate is l, the width of the smallest layer is $l/81$ and the thickness of the plate is $2h$. The width of the plate is d (Fig.1). The square defects are composed of aluminum (longitudinal velocities 6 260ms^{-1} and density 2700 kg·m^{-3}). The location and the rotation angle θ with respect to Ox_1 of these defects are known. The defects are oriented with respect to $\theta = 30^{\circ}$ with respect to Ox_1.

The piezoelectric material is characterized by two second-order elastic constants, three third-order elastic constants, two (linear and nonlinear) dielectric constants and two (linear and nonlinear) coefficients of piezoelectricity [31–33]. Throughout the paper, repeated indices denote summation over the range (1, 2, 3). An index followed by a comma represents partial differentiation with respect to space variables and a superposed dot indicates differentiation with respect to time.

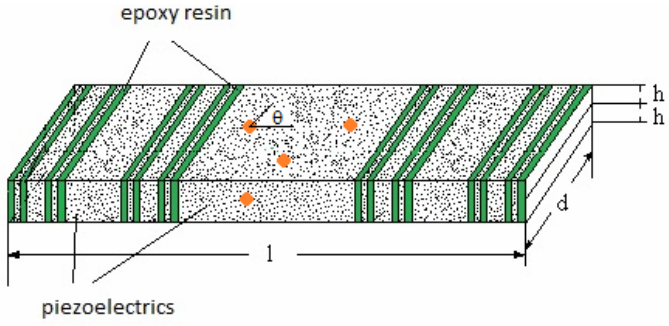

Fig. 1 – The plate with Cantor-like structure with four square defects.

The calculus is carried out for $l =$ 67.5 mm and $2h = 0.3$ mm. The eigenfrequencies for the film with and without defects are shown in Table 1 and Table 2, respectively. We see that as the angle θ is increasing, the computed eigenfrequencies very little increase, to a maximum one degree. The results indicate that the position of the localized modes is independent of the orientation of the square defects in the film.

Table 1

Computed eigenfrequencies for the film without defects

$\omega/2\pi$	100.2 $\pm$ 0.05	167 $\pm$ 0.01	217.1 $\pm$ 0.03	250.5 $\pm$ 0.1	334 $\pm$ 0.1	367.4 $\pm$ 0.05	417.5 $\pm$ 0.1	501 $\pm$ 0.02	584.5 $\pm$ 0.1

Table 2

Computed eigenfrequencies for the film with defects with respect to θ

$\omega/2\pi$	100.2 $\pm$ 0.05	167 $\pm$ 0.01	217.1 $\pm$ 0.03	250.5 $\pm$ 0.1	334 $\pm$ 0.1	367.4 $\pm$ 0.05	417.5 $\pm$ 0.1	501 $\pm$ 0.02	584.5 $\pm$ 0.1
$\theta =$ 5°	100.2 $\pm$ 0.05	167,2 $\pm$ 0.01	217.1 $\pm$ 0.03	250.5 $\pm$ 0.1	334.1 $\pm$ 0.1	367.6 $\pm$ 0.05	417.6 $\pm$ 0.1	501.3 $\pm$ 0.02	584.9 $\pm$ 0.1
$\theta = 15°$	100.2 $\pm$ 0.05	167,4 $\pm$ 0.01	217.3 $\pm$ 0.03	250.7 $\pm$ 0.1	334.2 $\pm$ 0.1	367.7 $\pm$ 0.05	417.9 $\pm$ 0.1	501.5 $\pm$ 0.02	585.1 $\pm$ 0.1
$\theta = 25°$	100.25 $\pm$ 0.05	167,5 $\pm$ 0.01	217.7 $\pm$ 0.03	250.8 $\pm$ 0.1	334.3 $\pm$ 0.1	367.9 $\pm$ 0.05	418.2 $\pm$ 0.1	501.6 $\pm$ 0.02	585.2 $\pm$ 0.1
$\theta = 35°$	100.33 $\pm$ 0.05	167,5 $\pm$ 0.01	218.0 $\pm$ 0.03	251.2 $\pm$ 0.1	334.7 $\pm$ 0.1	368.1 $\pm$ 0.05	418.3 $\pm$ 0.1	501.7 $\pm$ 0.02	585.3 $\pm$ 0.1
$\theta = 45°$	100.38 $\pm$ 0.05	167.8 $\pm$ 0.01	218.0 $\pm$ 0.03	251.4 $\pm$ 0.1	334.9 $\pm$ 0.1	368.2 $\pm$ 0.05	418.4 $\pm$ 0.1	501.8 $\pm$ 0.02	585.4 $\pm$ 0.1

The structure and size of the band-gap depend on $\bar{E}^0$. If $\bar{E}^0$ is increased above a threshold value $\bar{E}^0_{th} = 5.27$V the $\omega/2$ subharmonic generation is observed [31]. Note that Alippi *et al*. [28] obtain in the Cantor-like sample typical values of the lowest threshold voltages of 3–5 V. The amplitude of waves at the surface of the plate is function of $\bar{E}^0$.

The result of superposition of normal and subharmonic modes is the generation of two kind of vibration regimes: a localised-mode (fracton) regime and an extended-vibration (phonon) regime [31]. The fracton vibrations are mostly localised on a few elements, while the phonon vibrations essentially extend to the whole film. In the case of a periodical film the dispersion prevents good frequency matching between the fundamental and appropriate subharmonic modes. The results show that the defects cancel wave in the central area, a little more than if no defects are in the film, and in the rest of areas the wave picture is little altered and the symmetry disappears. The fracton mode is found mostly near the eigenfrequencies in both cases. The band structure for the wave propagation in direction Ox_1 is displayed in Fig. 2, for the film without/with defects, respectively. Defects change the aspect of the waves in the central area, and in the rest of areas the propagation picture is the same. The reduced unit of frequency is $\omega a/2\pi c_0$ with c_0 the speed of sound in air. We draw from Fig. 2 the conclusion that the size of the band-gap is favoured by the presence of defects. The band-gap area is large and compact. We remember that in the band-gap zone the film can prohibit the propagation of Lamb waves in Ox_1 direction.

It seems that the orientation of the square defects has no effect on the Lamb band structure. We have increased the number of defects in the central area to 45. The strange observation is that for a number of defects greater than 45, the size of the band-gap is decreases sharply. In addition, the compactness of the bad-gap deteriorates, as seen in Fig. 3. The incident and scattered acoustic pressure (amplitude) of the filme is presented in Fig. 4a, b for both cases, with and without defects oriented with respect to 30^0 with respect to Ox_1. The incident sound pulse impinges perpendicularly the film. The comparison of both maps confirms the acoustical reduction role of defects.

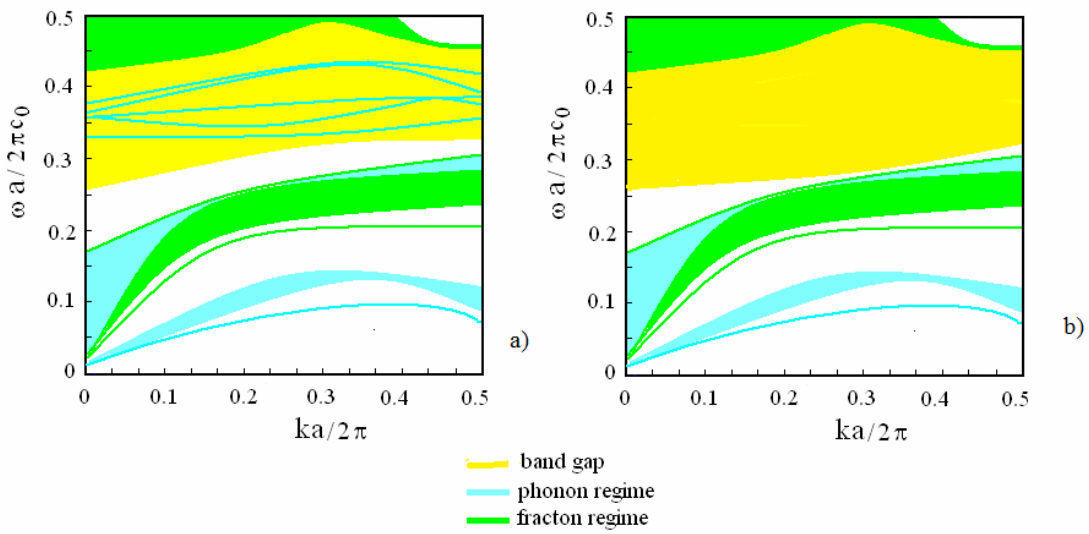

Fig. 2 – The Lamb band structures for the film:
a) without defects, b) with defects.

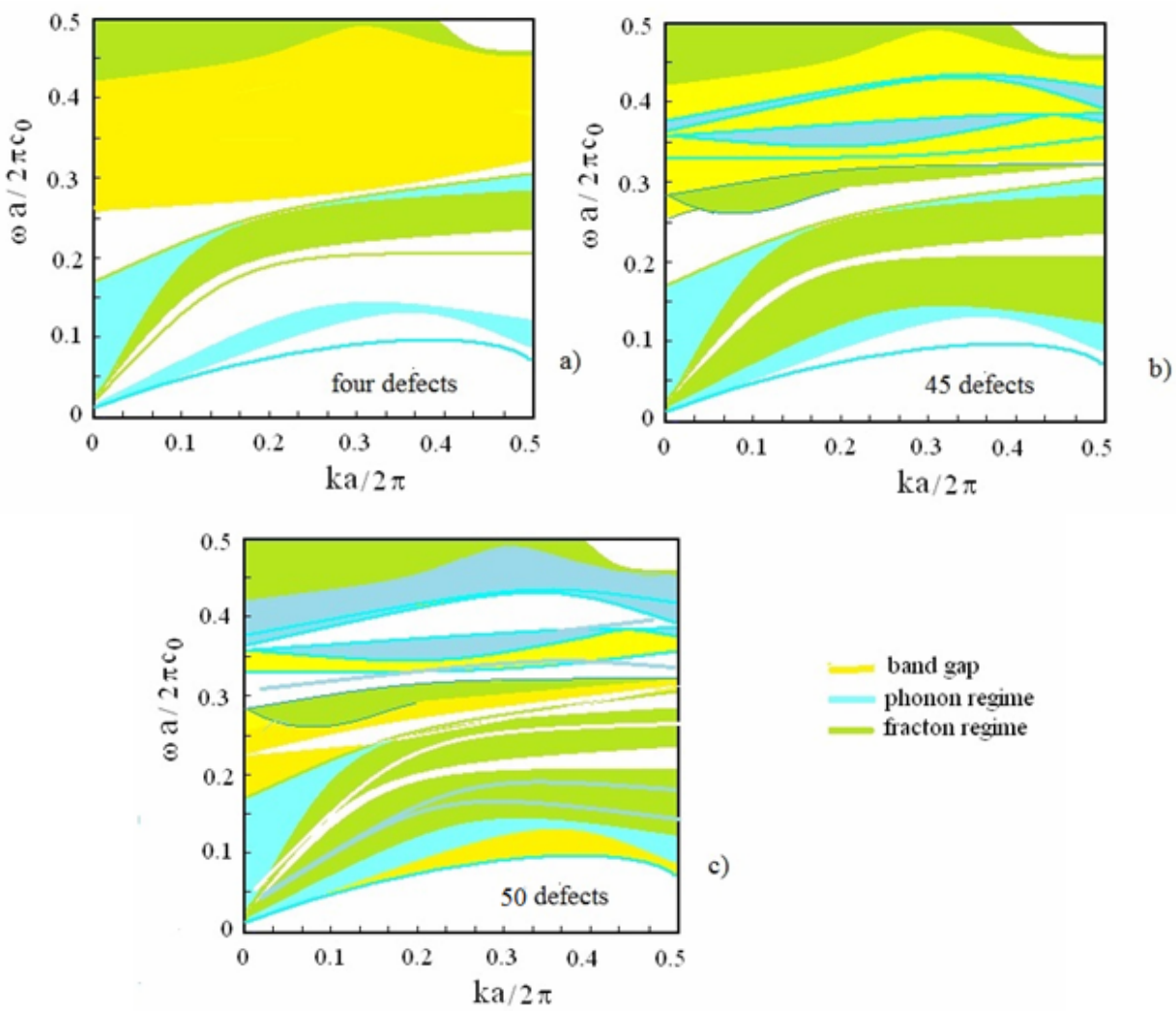

Fig. 3 – The Lamb band structures for the film:
a) four defects, b) 45 defects, c) 50 defects.

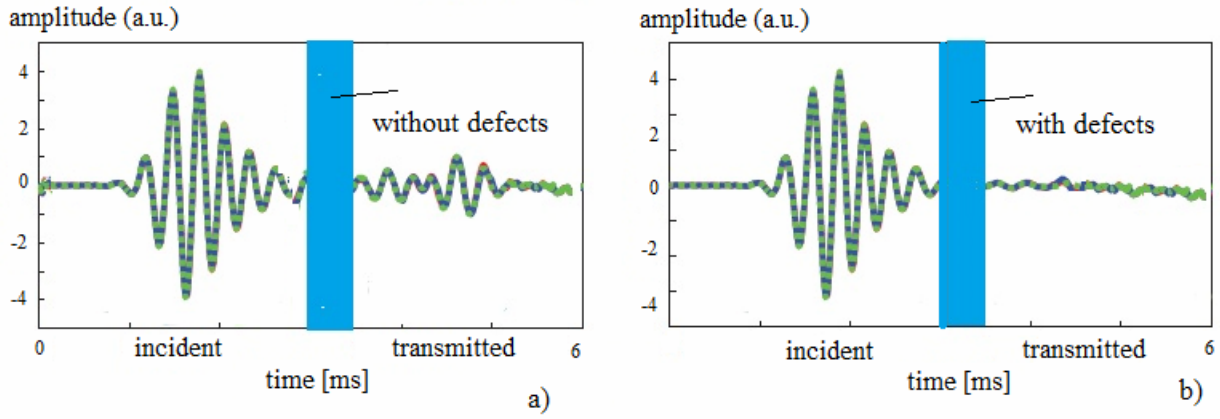

Fig 4 – Acoustic pressure (amplitude) of the scattering of the Lamb waves, impinging perpendicularly the film: a) film without defects, b) film with defects.

3. CONCLUSIONS

In this paper, the cnoidal method is applied to solve the problem of a multilayer film with square defects in order to discern some features of sonic composites, and how these defects influence the full band-gaps and localized modes. The defects have as result more favourable frequencies and spatial matching of coupled modes, leading to widening of the full band gaps. The position of the localized modes is independent of the orientation of the square defects in the film. In addition, the orientation of the square defects has no effect on the Lamb band structure. A strange observation appeared when the number of defects is greater than 45. In this case, the size of the band-gap is decreases sharply and the compactness of the bad-gap deteriorates. We suppose that these characteristics of the localized modes of the square defects are interested to the research on directional sonic filters and narrowband sonic waveguides.

ACKNOWLEDGEMENTS

The authors gratefully acknowledge the financial support of the National Authority for Scientific Research ANCS/UEFISCDI through the through the project PN-II-ID-PCE-2012-4-0023, Contract nr. 3/2013. The authors acknowledge the similar and equal contributions to this article.

REFERENCES

1. A.R. OSBORNE, *Soliton physics and the periodic inverse scattering transform*, Physica D, **86**, pp. 81–89, 1995.
2. B.A. DUBROVIN, V.B. MATVEEV, S.P. NOVIKOV, *Nonlinear equations of Korteweg–de Vries type, finite zone linear operators, and abelian varieties*, Russ. Math. Surv., **31**, *1*, pp. 59–146, 1976.
3. M.J. ABLOWITZ, H. SEGUR, *Solitons and the inverse scattering transforms,* SIAM, Philadelphia, 1981.
4. M.J. ABLOWITZ, P.A. CLARKSON, *Solitons, nonlinear evolution equations and inverse scattering*, Cambridge Univ. Press, Cambridge, 1991.
5. L. MUNTEANU, ST. DONESCU, *Introduction to Soliton Theory: Applications to Mechanics*, Book Series *Fundamental Theories of Physics*, **143**, Kluwer Academic Publishers, 2004.
6. M.J. ABLOWITZ, H. SEGUR, *Solitons and the inverse scattering transforms*, SIAM, Philadelphia, 1981.
7. T. MIYASHITA, *Full band gaps of sonic crystals made of acrylic cylinders in air-numerical and experimental investigations*, Jpn. J. Appl. Phys., **41**, pp. 3170-1-3175, 2002.
8. J.V. SACHEZ-PEREZ, D. CABALLERO, R. MARTINEZ-SALA, C. RUBIO, J. SANCHEZ-DEHESA, F. MESEGUER, F. LLINARES, F. GALVEZ, *Sound attenuation by a two-dimensional array of rigid cylinders*, Phys. Rev. Lett., **80**, *24*, pp. 5325–5328, 1998.
9. C. RUBIO, D. CABALLERO, J.V. SÁNCHEZ-PÉREZ, R. MARTÍNEZ-SALA, J. SÁNCHEZ-DEHESA, F. MESEGUER, F. CERVERA, *The existence of full gaps and deaf bands in two-dimensional sonic crystals*, J. Lightwave Technol., **17**, *11*, pp. 2202–2207, 1999.

10. J.O. VASSEUR, P.A. DEYMIER, A. KHELIF, P. LAMBIN, B. DJAFARI- ROUHANI, A. AKJOUJ, L. DOBRZYNSKI, N. FETTOUHI, J. ZEMMOURI, *Phononic crystal with low filling fraction and absolute acoustic band gap in the audible frequency range: A theoretical and experimental study*, Phys. Rev. E, **65**, pp. 056608–056614, 2002.
11. C. GOFFAUX, F. MASERI, J.O. VASSEUR, B. DJAFARI-ROUHANI, P. LAMBIN, *Measurements and calculations of the sound attenuation by a phononic band gap structure suitable for an insulating partition application*, Appl. Phys. Lett., **83**, pp. 281–283, 2003.
12. C. GOFFAUX, J. SANCHEZ-DEHESA, *Two-dimensional phononic crystals studied using a variational method: application to lattices of locally resonant materials*, Phys. Rev. B , **67**, pp. 144301, 2003.
13. B.C. GUPTA, Z. YE, *Theoretical analysis of the focusing of acoustic waves by two-dimensional sonic crystals*, Phys. Rev. E, **67**, pp. 036603, 2003.
14. I.E. PSAROBAS, N. STEFANOU, A. MODINOS, *Scattering of elastic waves by periodic arrays of spherical bodies*, Phys. Rev. B, **62**, *1*, pp. 278–291, 2000.
15. Z. LIU, X. ZHANG, Y. MAO, Y.Y. ZHU, Z. YANG, C.T. CHAN, P. SHENG, *Locally resonant sonic materials*, Science, **289**, pp. 1734–1736, 2000.
16. T. MIYASHITA, R. TANIGUCHI, H. SAKAMOTO, *Experimental full band-gap of a sonic-crystal slab structure of a 2D lattice of aluminum rods in air*, Proc. 5th World Congress on Ultrasonics TO-PM04.02, 2003.
17. M. HIRSEKORN, P.P. DELSANTO, N.K. BATRA, P. MATIC, *Modelling and simulation of acoustic wave propagation in locally resonant sonic materials*, Ultrasonics, **42**, pp. 231–235, 2004.
18. J.D. JOANNOPOULOS, S.G. JOHNSON, J.N. WINN, R.D. MEADE, *Photonic Crystals*, Princeton University Press, Second Edition, 2008.
19. Y. ZHAO, L.B..YUAN, *Characteristics of multi-point defect modes in 2D photonic crystals*, J. Phys. D: Appl. Phys., **42**, *1*, pp. 015403, 2009.
20. Y. ZHAO, Y.B. WU, L.B., YUAN, *Characteristics of the localized modes in 2D photonic crystal with heterostructure point defect*, Phys. Scr., **80**, pp. 065401, 2009.
21. F. WU, Z. HOU, Z. LIU, T. LIU, *Point defect states in two-dimensional phononic crystals*, Phys. Lett. A, **292**, 198, 2001.
22. R. SAINIDOU, N. STEFANOU, *Guided and quasiquided elastic waves in phononic crystal slabs*, Phys. Rev. B, **73**, pp. 184301, 2006.
23. M. GEI, *Elastic waves guided by a material interface*, European Journal of Mechanics-A/Solids, **27**, *3*, pp. 328–345, 2008.
24. V. LAUDE, Y. ACHAOUI, S. BENCHABANE, A. KHELIF, *Evanescent Bloch waves and the complex band structure of phononic crystals*, Phys. Rev. B, **80**, pp. 092301, 2009.
25. V. ROMERO-GARCÍA, J.V. SÁNCHEZ-PÉREZ, L.M. GARCIA-RAFFI, *Evanescent modes in sonic crystals: Complex relation dispersion and supercell approximation*, Journal of Applied Physics, **108**, *4*, pp. 108–113, 2010.
26. L.MUNTEANU, V. CHIROIU, V. SERBAN, *From geometric transformations to auxetic materials*, CMC: Computers, Materials & Continua, **42**, *3*, pp. 175–203, 2014.
27. L. MUNTEANU, V. CHIROIU, ST. DONESCU, C. BRIŞAN, *A new class of sonic composites*, Journal of Applied Physics, **115**, pp. 104904, 2014.
28. L. MUNTEANU, V. CHIROIU, *On the dynamics of locally resonant sonic composites*, European Journal of Mechanics-A/Solids, **29**, *5*, pp. 871–878, 2010.
29. V. CHIROIU, C. BRIŞAN, M.A. POPESCU, I. GIRIP, L. MUNTEANU, *On the sonic composites without/with defects*, Journal of Applied Physics, **114**, *16*, pp. 164909-1-10, 2013.
30. G. CHATZIGEORGIOU, A. JAVILI, P. STEINMANN, *Multiscale modeling for composites with energetic interfaces at the micro or nanoscale*, Mathematics and Mechanics of Solids, 1081286513516122, 2013.
31. L. MUNTEANU, V. CHIROIU, T. SIRETEANU, D. DUMITRIU, *A multilayer sonic film*, Journal of Applied Physics, **118**, 165302, 2015.
32. A. ALIPPI, *Nonlinear acoustic propagation in piezoelectric crystals*, Ferroelectrics, **42**, pp. 109–116, 1982.
33. A. ALIPPI, G. SHKERDIN, A. BERTTUCCI, F. CRACIUN, E. MOLINARI, A. PETRI, *Threshold lowering for sub-harmonic generation in Cantor composite structures*, Physica A, **191**, *1–4*, pp. 540–544, 1992.
34. A. ALIPPI, F. CRACIUN, E. MOLINARI, *Stopband edges in the dispersion curves of Lamb waves propagating in piezoelectric periodical structures*, Appl. Phys. Lett., **53**, *19*, p. 1805, 1988.
35. F. CRACIUN, A. BETTUCCI, E. MOLINARI, A. PETRI, A. ALIPPI, *Direct experimental observation of fracton mode patterns in one-dimensional Cantor composites*, Phys. Rev. Lett., **68**, *10*, 1992.
36. M. SCALERANDI, P.P. DELSANTO, C. CHIROIU, V. CHIROIU, *Numerical simulation of pulse propagation in nonlinear 1-D media*, Journal of the Acoustical Society of America, **106**, pp. 2424–2430, 1999.
37. V. CHIROIU, P.P. DELSANTO, M. SCALERANDI, C. CHIROIU, T. SIRETEANU, *Subharmonic generation in piezoelectrics with Cantor-like structure*, Journal of Physics D: Applied Physics, Institute of Physics Publishing, **34**, *3*, pp. 1579–1586, 2001.

Received September 6, 2016